Thermal Characterization of Energy Pile Dynamics

Paolo Conti(✉), Eva Schito, and Daniele Testi

Department of Energy, Systems, Territory and Constructions Engineering (DESTEC), University of Pisa, 56122 Pisa, Italy
paolo.conti@unipi.it

Abstract. The heat transfer process in energy piles is strongly affected by the heat capacity of such foundation elements. This phenomenon is more pronounced for energy piles compared to borehole heat exchangers, because of the lower slenderness of the former compared to the latter, and involves axial thermal gradients. In literature, capacity effects of energy piles and their transient thermal performance have not been analysed in depth. Looking at such challenge, this paper investigates the dynamic thermal performance of energy piles at short-to-medium time scales. The work analyses the results of almost thirty 3D finite element simulations of an energy pile equipped with 3-U ducts by varying: (i) the velocity of the fluid circulating in the ducts, (ii) the slenderness ratio of the pile, (iii) the radial position of the ducts, and (iv) the boundary condition characterizing the uppermost surface of the model. Simulation results are analysed to identify for which times, geometries, and operative conditions the energy pile can be modelled with a 2D geometry, instead of a full 3D geometry. Our analysis highlights a limited relevance of the axial effects during the transient period in any tested configuration. These results are functional to the application of simplified analytical models and design criteria for energy piles.

1 Introduction

Energy piles (EPs) represent a promising solution to reduce the installation costs of GSHP systems, mainly because the heat exchanging pipes are embedded in the building foundations without significant additional costs with respect to the already-needed expenditure for geo-mechanical requirements (Fadejev et al. 2017; Batini et al. 2015). However, the EP design and performance assessment are ongoing multi-disciplinary and mechanical-thermal issues (Rotta Loria and Laloui 2016).

The thermal modelling of an EP is difficult for several reasons, e.g., EPs cannot be assumed as slender bodies, the heat transfer process is affected by the large heat capacity of the foundation or by possible interaction with outdoor climate and/or overhead buildings (Conti et al. 2016; Li and Lai 2015). However, an accurate EP model is fundamental for a proper analysis of the system, as ground-coupled heat exchangers are one of the main drivers of the overall GSHP performance (Casarosa et al. 2014).

A. Ferrari and L. Laloui (Eds.): SEG 2018, SSGG, pp. 123–131, 2019.
https://doi.org/10.1007/978-3-319-99670-7_16

At present, EPs are modelled through numerical methods and software as, to the best of our knowledge, there are no established dynamic analytical models (Fadejev et al. 2017; Zarrella et al. 2013). With respect to numerical methods, analytical approaches are attractive alternatives, representing an appropriate trade off among implementation efforts, computational time, and solution accuracy (Conti 2016, 2017; Conti et al. 2016). On the other hand, the development of new analytical methods always requires some simplification assumptions, to be verified through numerical or experimental analyses. For instance, the composite-medium line-source model (Li and Lai 2012) refers to the 2D thermal field evolution due to a linear thermal source located in composite cylindrical media, and it is potentially applicable to simulate EP thermal dynamics, provided that the 2D assumption is verified.

In this paper, we analyse the transient period of an EP to figure out the duration and the characteristics of the thermal field evolution at short-to-medium time scales. Specifically, we run 36 simulations varying geometrical parameters and operative conditions. We focus on two main points: the duration of transient period, the relevance of the thermal gradients over the axial direction with respect to the radial dimension. The findings will be functional to the application of the composite-medium line-source model in the EP context.

2 Description of the Numerical Model

The numerical analysis was performed through the widespread commercial software COMSOL Multiphysics® (COMSOL 2015). We performed 36 full transient 3D FEM simulation of a reference 3-U energy pile, varying the position of the U-loops, the flow rate within the ducts, the aspect ratio of the pile, and the upper boundary condition of the numerical domain from adiabatic to isothermal (see Table 1 and Fig. 1). All the media were assumed to be as constant-property, homogeneous, isotropic, and purely conductive. The ducts are assumed as purely thermal resistances, with a negligible thermal capacity. The thermal conductivity, λ, of the ground, EP concrete, and ducts are 1.5, 2.1, and 0.4 W/(m K), respectively. Thermal diffusivity α of the ground and EP concrete are 0.6 and 1.0 mm^2/s, respectively.

The heat transfer over the EP concrete and the ground are modelled through the classical heat equation based on the Fourier's law. The circulating fluid is assumed as water and it is modelled through a 1-D energy equation along the geometry edges representing the ducts (see Fig. 2):

$$\rho_f c_f \frac{\partial \theta_f}{\partial t} + \rho_f c_f u_f \frac{\partial \theta_f}{\partial s} = \lambda_f \nabla^2 \theta_f + \dot{q}_p / \left(\pi r_{p,i}^2 \right) \tag{1}$$

where s is curvilinear coordinate and $\dot{q}_p = 2\pi r_{p,i} U_p \left(\theta_{p,ext} - \theta_f \right)$. $\theta_{p,ext}$ is the local temperature of the duct-pile interface. The overall heat transfer coefficient, U_p includes the convective fluid-duct thermal resistance and the conductive duct thermal resistance. Further details can be found in Batini et al. (2015).

The actual number of mesh elements depends on the specific simulation. As general rule, we used a swept method over the EP axial direction and an unstructured triangular

Table 1. Parameters of tested configurations (r = 0.45 m)

Conf. #	U-loops arrangement	Pipes radial position [m]	Pile depth, H [m]	Fluid velocity, u_f [m/s]	Aspect ratio, $H/(2r_b)$ [–]	Boundary condition (B.C.)	$\tau_{\bar{\theta}_f}$ [s]	τ_p [s]	$\alpha_b \tau_b / r_b^2$
1	Type A	0.13	9	0.2	10	Isothermal	45	404	2.21
2	Type A	0.13	9	0.5	10	Isothermal	18	263	2.21
3	Type A	0.13	9	1	10	Isothermal	9	198	2.21
4	Type A	0.13	36	0.2	40	Isothermal	178	999	2.48
5	Type A	0.13	36	0.5	40	Isothermal	72	526	2.48
6	Type A	0.13	36	1	40	Isothermal	36	378	2.48
7	Type A	0.40	9	0.2	10	Isothermal	45	404	1.97
8	Type A	0.40	9	0.5	10	Isothermal	18	267	1.97
9	Type A	0.40	9	1	10	Isothermal	9	199	1.97
10	Type A	0.40	36	0.2	40	Isothermal	178	989	2.21
11	Type A	0.40	36	0.5	40	Isothermal	72	521	1.97
12	Type A	0.40	36	1	40	Isothermal	36	378	1.97
13	Type B	0.13	9	0.2	10	Isothermal	45	452	2.48
14	Type B	0.13	9	0.5	10	Isothermal	18	277	2.48
15	Type B	0.13	9	1	10	Isothermal	9	199	2.48
16	Type B	0.13	36	0.2	40	Isothermal	178	1293	2.78
17	Type B	0.13	36	0.5	40	Isothermal	72	640	2.46
18	Type B	0.13	36	1	40	Isothermal	36	429	2.48
19	Type B	0.40	9	0.2	10	Isothermal	45	410	2.21
20	Type B	0.40	9	0.5	10	Isothermal	18	269	2.21
21	Type B	0.40	9	1	10	Isothermal	9	201	2.21
22	Type B	0.40	36	0.2	40	Isothermal	178	994	2.48
23	Type B	0.40	36	0.5	40	Isothermal	72	524	2.48

(*continued*)

Table 1. (*continued*)

Conf. #	U-loops arrangement	Pipes radial position [m]	Pile depth, H [m]	Fluid velocity, u_f [m/s]	Aspect ratio, $H/(2r_b)$ [–]	Boundary condition (B.C.)	$\tau_{\bar{\theta}_f}$ [s]	τ_p [s]	$\alpha_b \tau_b / r_b^2$
24	Type B	0.40	36	1	40	Isothermal	36	384	2.48
25	Type A	0.30	28	0.2	31.1	Isothermal	138	797	1.97
26	Type A	0.30	28	0.2	31.1	Adiabatic	138	797	1.97
27	Type A	0.30	9	0.2	10	Isothermal	45	383	1.75
28	Type A	0.30	9	0.2	10	Adiabatic	45	370	1.97
29	Type A	0.30	36	0.2	40	Isothermal	178	966	1.97
30	Type A	0.30	36	0.2	40	Adiabatic	178	966	1.97
31	Type A	0.30	28	0.5	31.1	Isothermal	56	443	1.75
32	Type A	0.30	28	0.5	31.1	Adiabatic	56	443	1.97
33	Type A	0.30	9	0.5	10	Isothermal	18	262	1.75
34	Type A	0.30	9	0.5	10	Adiabatic	18	262	1.75
35	Type A	0.30	36	0.5	40	Isothermal	72	526	1.97
36	Type A	0.30	36	0.5	40	Adiabatic	72	526	1.97

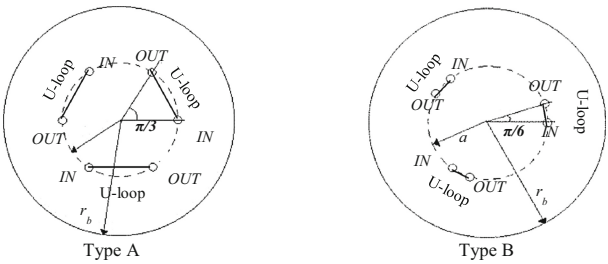

Fig. 1. Tested arrangements for U-loops. Type B refers to a closer position of the U legs.

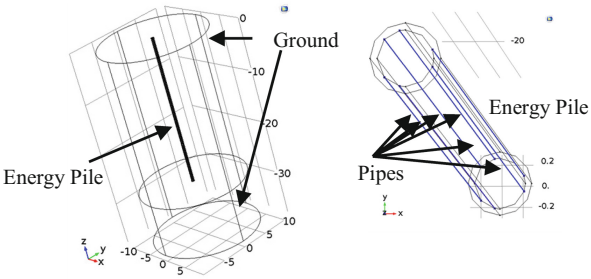

Fig. 2. Numerical domain (images from COMSOL Multiphysics GUI). The six blue lines represent the ducts embedded in the energy pile.

mesh on the upper surface (see Fig. 3). The maximum size of the triangular elements is 0.02 m within the pile and 3.3 m in the soil. The maximum height of the prisms is 3.1 m. The simulated period consists of 20 days divided in a logarithmically-spaced vector of pace $\log_{10}(\tau^n/\tau^{n-1}) = 0.05$. We used an intermediate backward differentiation formula as time-integration method (COMSOL 2015).

3 Results: Characteristic Periods and Axial Thermal Gradients

According to Li and Lai (2015), the heat transfer process in vertical ground-coupled heat exchangers (EPs included) can be split into three separate characteristic periods. The first period, $\tau < \tau_p$ refers to the fluid and ducts thermal dynamics. We define τ_p, as the time after which the heat exchange through the pipes is practically equivalent to the enthalpy variation of the fluid between the inlet and the outlet sections. The term "practically equivalent" refers to a relative deviation lower than 5%. To better quantify τ_p, we wrote a simplified energy equation of the fluid with a lumped-parameters approach, namely:

$$\tau_{\bar{\theta}_f} = \rho_f c_f V_f \big/ \left(2\dot{m}_{f,p} c_f + US\right) \tag{2}$$

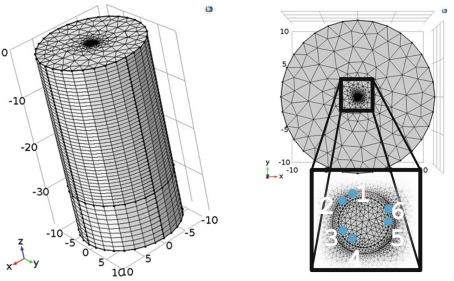

Fig. 3. Finite element mesh used in the simulations (images from COMSOL Multiphysics GUI). The position and the numbering of the ducts are highlighted in white.

where the mean operator refers to the arithmetic mean of the considered variable between the inlet and the outlet sections of a single U-loop. we expect that $\overline{\theta_f}$ reaches the steady-state value at a time proportional to the time constant of Eq. 2, $\tau_{\bar{\theta}_f} = \rho_f c_f V_f / \left(2\dot{m}_{f,p} c_f + US\right)$. The results shown in Fig. 4 confirms that $\tau_{\bar{\theta}_f}$ and τ_p are linearly dependent each other, according to a proportional factor of about 4. In Fig. 4 we see less than 36 markers as the others are overlapped to those with the same $\tau_{\bar{\theta}_f}$. In other words, the radial position of the pipes and the aspect ratio of the pile do not affect the dynamics of the circulating fluid at those short time scales $\tau < \tau_p$. We did not investigate shorter $\tau_{\bar{\theta}_f}$ as this would correspond to unrealistic high EP flow rate values.

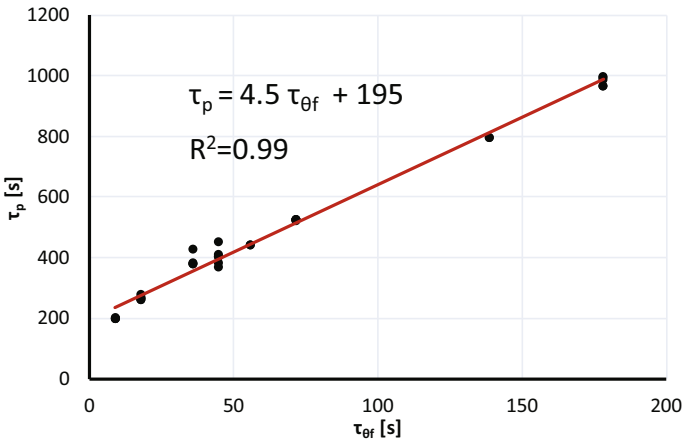

Fig. 4. Linear regression of τ_p as a function of the time constant $\tau_{\bar{\theta}_f}$.

The second period, $\tau_p < \tau < \tau_b$, refers to the thermal dynamics of the pile and it is driven by the heat capacity of the foundation. We can define τ_b as the time after which the thermal power exchanged through the ducts is practically equivalent to the thermal power exchanged through the pile-soil interface. Again, the term "practically equivalent" refers to a relative deviation lower than 5%. Table 1 shows the τ_b values for the

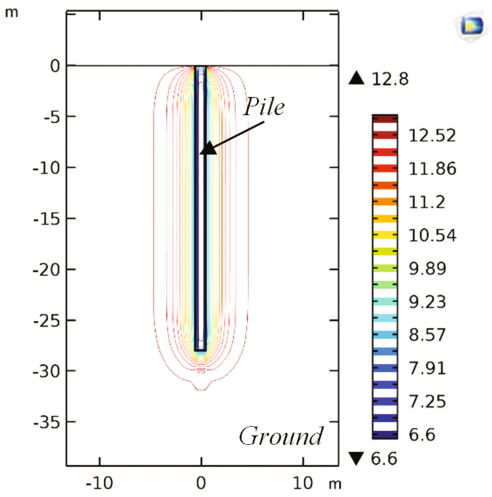

Fig. 5. Example of isothermal lines during the EP dynamics.

36 tested configurations, pointing also out that this value is approximately 2÷2.5 times the characteristic time of the pile, r_b^2/α_b. At $\tau > \tau_b$, namely the third period, the pile becomes a purely-resistance body and it can be modelled through the classical *borehole thermal resistance*, R_b (Conti et al. 2016).

The thermal dynamics of an EP occurs in the above-described second period. Figure 5 shows an example of the typical isothermal lines during that dynamics.

Those lines are practically parallel to the pile axis, hinting that no heat transfer occurs in axial direction. However, to better quantify the relevance of the heat conduction over the axial direction, we analysed the numerical results in term of thermal power over cross-axial surfaces at different depth z, namely:

$$\left|\dot{Q}_z\right|(z) = \int_0^{r_b}\int_0^{2\pi} |\dot{q}_z| r dr d\varphi = \int_0^{r_b}\int_0^{2\pi} \left|-\lambda_b \frac{\partial\theta}{\partial z}\right| r dr d\varphi \tag{3}$$

$\left|\dot{Q}_z\right|$ is not an actual quantification of the thermal performances of the pile, but it provides a reasonable indication on the entity of thermal flux over the axial direction. If it would result sufficiently small with respect to the enthalpy drop of the fluid, $\dot{Q}_p$, we can conclude that the heat conduction mainly occurs over the axial direction. Figure 6 show the evolution of $\left|\dot{Q}_z\right|/\left|\dot{Q}_p\right|$ values for all the tested configurations over the simulated 20 days. We note that $\left|\dot{Q}_z\right|/\left|\dot{Q}_p\right|$ is always practically null in the middle of the pile, with some "edge effects" on the top and bottom of the pile only for the shallow geometry (aspect ratio $H/2r_b < 10$). In any case, there are no significant effects of uppermost boundary conditions, flow rate and radial position of the ducts. We conclude that the transient periods for typical EP geometries can be analysed and modelled with a 2D approach.

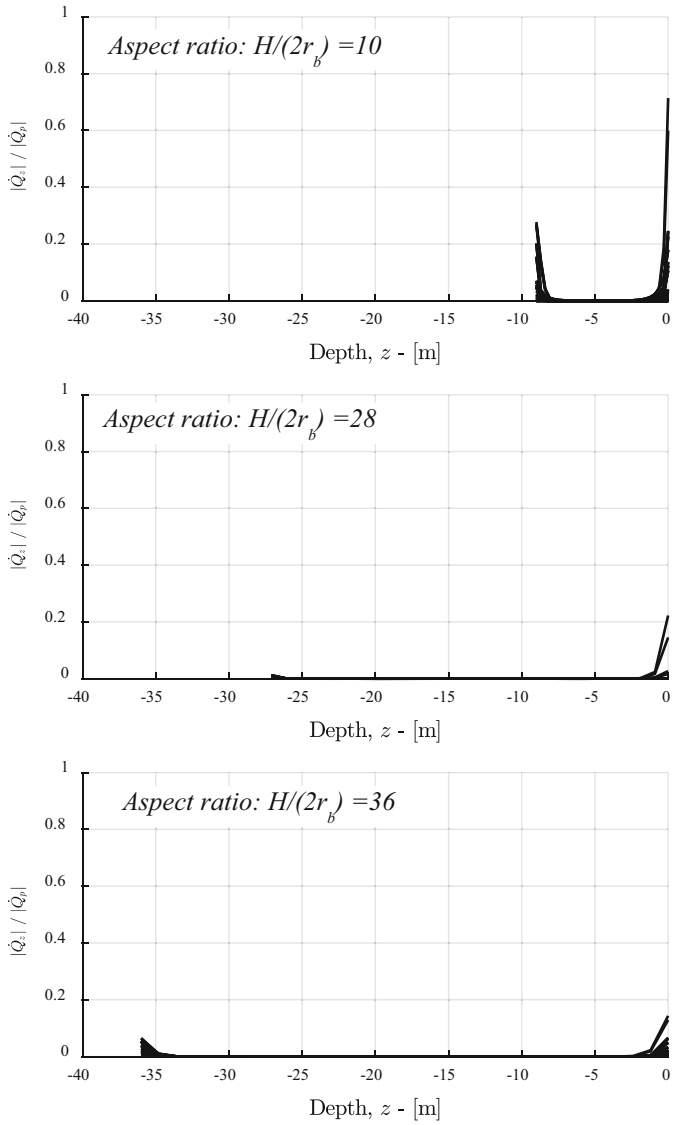

Fig. 6. 20-day evolution of the $|\dot{Q}_z|/|\dot{Q}_p|$ ratio for all tested configurations.

4 Conclusions

The paper analysed 36 full transient 3D FEM simulations, varying geometrical and operative conditions of a reference EP. We found the following limits for the three characteristic periods of the heat transfer in a single EP. The first one ends at four times the time constant of the fluid energy equation (see Eq. 2 and Fig. 4). The second

period, the most relevant for the dynamic performance, ends at 2÷3 times the dimensionless time, r_b^2/α_b, with a minor influence of the radial ducts position, aspect ratio of the pile, flow rate and uppermost boundary condition. Additionally, for the most of simulations the heat transfer was found mainly to occur in the radial direction, thus making possible a 2D modelling for typical EP geometries (i.e. $H/(2r_b) > 10$) during that second period. Future analyses concern the influence of the fluid flow rate and R_b on the axial thermal gradient.

Those results are functional to the application of simplified analytical methods, such as the composite-medium line-source model, which can be successfully employed in dynamic simulations and optimization codes to seek the best sizing, operation strategy, and RES integration for UTES and GSHP (Grassi et al. 2015).

References

Batini, N., Rotta Loria, A.F., Conti, P., Testi, D., Grassi, W., Laloui, L.: Energy and geotechnical behaviour of energy piles for different design solutions. Appl. Therm. Eng. **86**, 199–213 (2015). https://doi.org/10.1016/j.applthermaleng.2015.04.050

Casarosa, C., Conti, P., Franco, A., Grassi, W., Testi, D.: Analysis of thermodynamic losses in ground source heat pumps and their influence on overall system performance. J. Phys: Conf. Ser. **547**, 012006 (2014). https://doi.org/10.1088/1742-6596/547/1/012006

COMSOL Multiphysics® v. 5.2. www.comsol.com. COMSOL AB, Stockholm, Sweden (2015)

Conti, P.: Dimensionless maps for the validity of analytical ground heat transfer models for GSHP applications. Energies **9**, 890 (2016). https://doi.org/10.3390/en9110890

Conti, P., Testi, D., Grassi, W.: Revised heat transfer modeling of double-U vertical ground-coupled heat exchangers. Appl. Therm. Eng. **106**, 1257–1267 (2016). https://doi.org/10.1016/j.applthermaleng.2016.06.097

Conti, P., Testi, D., Grassi, W.: A brief compendium of correlations and analytical formulae for the thermal field generated by a heat source embedded in porous and purely-conductive media. J. Phys: Conf. Ser. **923**, 012056 (2017). https://doi.org/10.1088/1742-6596/923/1/012056

Fadejev, J., Simson, R., Kurnitski, J., Haghighat, F.: A review on energy piles design, sizing and modelling. Energy **122**, 390–407 (2017). https://doi.org/10.1016/j.energy.2017.01.097

Grassi, W., Conti, P., Schito, E., Testi, D.: On sustainable and efficient design of ground-source heat pump systems. J. Phys: Conf. Ser. **655**, 12003 (2015). https://doi.org/10.1088/1742-6596/655/1/012003

Li, M., Lai, A.C.K.: New temperature response functions (G functions) for pile and borehole ground heat exchangers based on composite-medium line-source theory. Energy **38**, 255–263 (2012). https://doi.org/10.1016/j.energy.2011.12.004

Li, M., Lai, A.C.K.: Review of analytical models for heat transfer by vertical ground heat exchangers (GHEs): a perspective of time and space scales. Appl. Energy **151**, 178–191 (2015). https://doi.org/10.1016/j.apenergy.2015.04.070

Rotta Loria, A.F., Laloui, L.: The interaction factor method for energy pile groups. Comput. Geotech. **80**, 121–137 (2016). https://doi.org/10.1016/j.compgeo.2016.07.002

Zarrella, A., De Carli, M., Galgaro, A.: Thermal performance of two types of energy foundation pile: helical pipe and triple U-tube. Appl. Therm. Eng. **61**, 301–310 (2013). https://doi.org/10.1016/j.applthermaleng.2013.08.011